Hydrogen as promoter and inhibitor of superionicity: A case study on Li-N-H systems

Andreas Blomqvist,[1] C. Moysés Araújo,[1,2] Ralph H. Scheicher,[1] Pornjuk Srepusharawoot,[1,3] Wen Li,[5] Ping Chen,[4,5,6] and Rajeev Ahuja[1,2,*]

[1]*Department of Physics and Astronomy, Uppsala University, P.O. Box 516, SE-751 20 Uppsala, Sweden*

[2]*Applied Materials Physics, Department of Materials and Engineering, Royal Institute of Technology (KTH), SE-100 44 Stockholm, Sweden*

[3]*Department of Physics, Faculty of Science, Khon Kaen University, 40002 Khon Kaen, Thailand*

[4]*Dalian Institute of Chemical Physics, Dalian 116023, People's Republic of China*

[5]*Department of Physics, National University of Singapore, 117542 Singapore, Singapore*

[6]*Department of Chemistry, National University of Singapore, 117543 Singapore, Singapore*

(Received 18 March 2010; revised manuscript received 7 July 2010; published 26 July 2010)

Materials which possess a high lithium ion conductivity are very attractive for battery and fuel cell applications. Hydrogenation of the fast-ion conductor lithium nitride (Li_3N) leads to the formation of lithium imide (Li_2NH) and subsequently of lithium amide ($LiNH_2$). Using *ab initio* molecular dynamics simulations, we carried out a comparative study of the Li diffusion in these three systems. The results demonstrate that hydrogen can work as both promoter and inhibitor of Li mobility, with the lowest transition temperature to the superionic state occurring in Li_2NH. Furthermore, we show that the creation of Li vacancies strongly affects Li diffusion in Li_3N, but not so in Li_2NH. Finally, we explain our findings with the help of a simple model.

DOI: 10.1103/PhysRevB.82.024304 PACS number(s): 61.20.Ja, 66.10.−x, 71.15.Mb, 71.15.Pd

I. INTRODUCTION

Solid-state systems possessing a high mobility of lithium ions are of tremendous interest for battery and fuel cell applications. As a consequence, the research into new materials with high lithium ion conductivity forms a very active field. Lithium nitride (Li_3N) is one such material in which lithium ions are known to exist in a highly mobile superionic state. Hydrogenation of this system leads to the formation of lithium imide[1] (Li_2NH) and subsequently of lithium amide[2] ($LiNH_2$), a process which has been proposed[3] and further investigated[4–12] for its merits in the field of hydrogen storage research.[13–20] Here we show from first principles that the step-wise addition of hydrogen to Li_3N can act both as a promoter and inhibitor of the superionic state, and propose a simple model to explain these surprising findings.

Li_3N itself is a prominent example of a superionic conductor, and as such it has naturally been the target of previous theoretical investigations. Unlike the present study, however, which is based on first principles, those earlier molecular dynamics (MD) simulations generally used pair potentials to determine the forces between the ions. For example, Wolf *et al.*[21,22] investigated the transport mechanisms in Li_3N at $T=300$ and 400 K, and succeeded in qualitatively reproducing the experimentally observed T-dependent anisotropic mobilities due to the distinct Li(1) and Li(2) sublattices.[21] From an analysis of the Li ion trajectories they derived the detailed transport mechanisms in Li_3N, which shows highly correlated migrations in the Li_2N plane. Eventually, for higher temperature, the interplanar interstitials were found to become more important for conduction.[22]

Very recently, *ab initio* path integral molecular dynamics simulations were combined with ^1H NMR experiments to investigate $LiNH_2$ and Li_2NH. The study[23] showed that Li atoms in these systems possess higher mobility and are more disordered than what is deduced from x-ray scattering data. This finding confirms our earlier conclusion[24] that time-averaging measurements (such as x-ray or neutron scattering) in Li_2NH will show Li sublattices with a well-ordered structure (i.e., simple-cubic), missing the presence of a superionic state.

II. METHODS

The approach and computational methods employed in the present study are very similar to those recently used by us[24] to show emergent superionicity in Li_2NH at around 400 K. Likewise, this study utilizes *ab initio* MD simulations, meaning that all forces were actually obtained from density functional theory (DFT)[25] as implemented in the Vienna *ab initio* simulation package (VASP).[26,27] Several other groups have also recently applied *ab initio* MD to study diffusion, as well as structural and vibrational properties in various hydrogen-rich systems,[28–31] showing that it can be a very useful and reliable computational tool. Our calculations are based on the generalized gradient approximation (GGA)[32] and made use of the projector-augmented wave (PAW) approach.[33] A cutoff energy of 700 eV was used throughout the simulations which were performed in the canonical ensemble (with volume, particle number, and temperature fixed).

All three systems (Li_3N, $LiNH_2$, and $LiNH_2$) were simulated at temperatures ranging from 200 to 700 K with incremental steps of 100 K. Each simulation was allowed to run for a total of 30000 1-fs time steps, except for the Li_3N and the $LiNH_2$ systems, when both contain a Li vacancy, which required 120 and 50 ps, respectively, to converge the diffusion coefficients. The first 10 ps were reserved for allowing the simulations equilibrating to the desired geometry at each given temperature and were discarded from the subsequent analysis. Within the equilibration time frame (0–10 ps), convergence with respect to total energy, velocities, forces, and

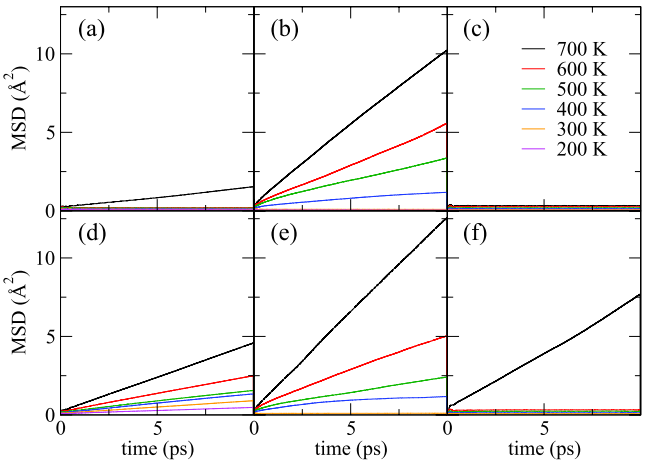

FIG. 1. (Color online) Mean square displacement (MSD) for Li ions as a function of time in (a) Li_3N, (b) Li_2NH, and (c) $LiNH_2$ with *no* Li vacancies. MSD with *one* Li vacancy in the supercell in (d) Li_3N, (e) Li_2NH, and (f) $LiNH_2$. Note that the scale on the y axis is identical in all six panels to facilitate comparisons.

positions was carefully checked. From the data time frame (after the initial 10 ps equilibration) we then extracted the target information in the form of mean square displacements, atomic trajectories, and bond orientation distributions. The convergence of diffusion coefficients with respect to simulation time was checked. All systems, except for the Li_3N and the $LiNH_2$ systems with a vacancy, were converged after 30 ps. The reason for the long simulation time required in the Li_3N and the $LiNH_2$ systems when both contain a vacancy, is that only one entity, namely, the vacancy, is diffusing compared to, e.g., Li_2NH where all 64 Li are the diffusing entities. The supercells constructed for Li_3N, Li_2NH, and $LiNH_2$ contain 108, 128, and 128 atoms, respectively.

In the case of Li_2NH, our tests revealed that the system retains no memory of the choice for the initial structure (as long as the latter is a reasonable choice) after the equilibration time of 10 ps has passed, so that all data extracted from the data time frame is unaffected by the particular structure chosen initially. This conveniently allowed us to avoid the ongoing debate about the correct low-temperature structures for Li_2NH. We have used the optimized structures of the $P6/mmm$ and $I\bar{4}$ phases for the initial structures of Li_3N and $LiNH_2$, respectively. Our calculated lattice parameters $a=3.64$ Å and $c=3.88$ Å for Li_3N, and $a=5.01$ Å and $c=10.31$ Å for $LiNH_2$ compare well with the experimental values of $a=3.637$ Å and $c=3.870$ Å for Li_3N,[34] and $a=5.034$ Å and $c=10.255$ Å for $LiNH_2$.[35]

III. RESULTS AND DISCUSSION

The temperature-dependent mean-square displacement (MSD) for Li ions in Li_3N, Li_2NH, and $LiNH_2$ is plotted as a function of time in Fig. 1. Zero-slope MSD curves indicate that Li stays essentially bound to its equilibrium site, with the finite height of the MSD level being attributed to the ion's vibrational amplitude, which is seen to rise with temperature. A finite-slope MSD curve is the telltale sign of

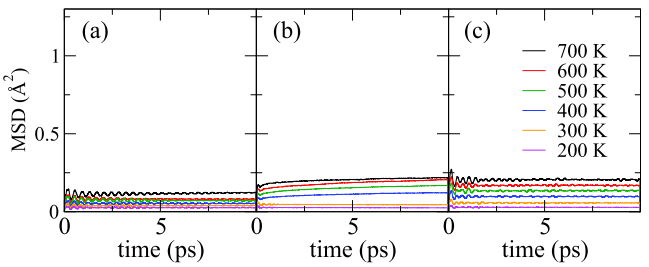

FIG. 2. (Color online) Mean-square displacement for nitrogen as a function of time in (a) Li_3N, (b) Li_2NH, and (c) $LiNH_2$. The scale on the y axis is identical in all three panels (note that the scale on the corresponding plots for Li in Fig. 1 is one order of magnitude larger). Effectively, almost all MSD curves are seen to run horizontal (zero slope), indicating that N stays bound to its respective equilibrium sites. Any parts of the curves which exhibit finite slope correspond presumably to a slight rearrangement of the anion sublattice.

diffusion taking place. Thus, in the case of Li_3N [Fig. 1(a)], it is clearly observed from the flat MSD curves for $T=200-600$ K that Li does not become mobile until the temperature has reached 700 K. For Li_2NH on the other hand, Li starts diffusing already at a comparatively low temperature of 400 K [Fig. 1(b)]. Finally, for $LiNH_2$, we find absolutely no mobility of Li in the studied temperature range [Fig. 1(c)]. It is important to note that for all three systems, the nitrogen atoms remain fixed to their respective equilibrium sites throughout the studied temperature range, as can be seen from Fig. 2. Thus, in those cases where Li becomes mobile, the system is truly in a superionic state. Our MD simulations therefore demonstrate that superionicity emerges already at a lower temperature in Li_2NH than in Li_3N (and is completely absent in $LiNH_2$).

Vacancies can of course have a big effect on the diffusion, and therefore we have also carried out MD simulations with Li-vacancies present in all three materials. Vacancies can be created in three different ways: (1) Frenkel defects, which we observed at 700 K in the Li_3N system, where one Li ion is pushed out from the Li_2N plane into the Li plane, allowing diffusion within the Li_2N plane, (2) nonstoichiometric growth conditions, and (3) applying an electric field to pull ions out of the material. To explicitly study the effect of the two latter possibilities, we have removed one Li atom in each of the three systems. It should be noted that the vacancy concentration will have a big influence on the magnitude of the diffusion; here, however, we are only interested in whether vacancies affect the diffusion or not. As can be seen from Fig. 1(d), a Li vacancy in Li_3N allows for the diffusion to start already below room temperature. In Li_2NH, there is virtually no effect on the MSD when introducing a Li vacancy [Fig. 1(e)], and no change in allowed temperature range for the diffusion can be observed from the coarse set of temperatures in our simulations. In $LiNH_2$ with one Li vacancy, we notice diffusion starting at a temperature of 700 K [Fig. 1(f)]. These results can be interpreted as follows: the Li sublattices in Li_3N and $LiNH_2$ require vacancies in order to allow for Li diffusion, while in Li_2NH, vacancies are apparently not a requirement. The slopes of the various MSD curves yield the diffusion coefficients which we plot as a

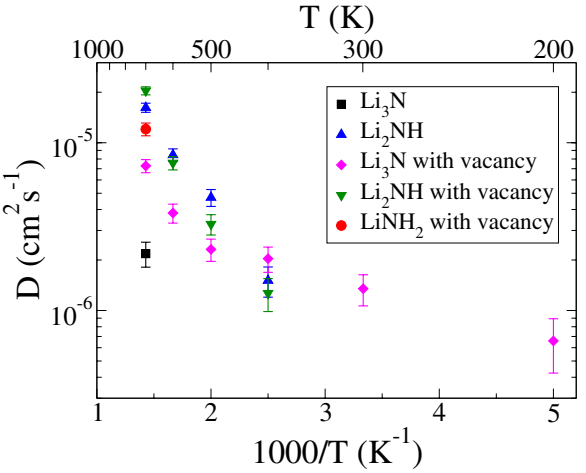

FIG. 3. (Color online) Plot of the diffusion coefficients calculated from the MSD for Li_3N (black squares), Li_2NH (blue triangle up), Li_3N with a Li vacancy (magenta diamonds), Li_2NH with a Li vacancy (green triangle down), and $LiNH_2$ with a Li vacancy (red circle).

function of temperature in Fig. 3. There it can also be seen very clearly that the introduction of vacancies does not noticeably enhance the diffusion of Li in Li_2NH. Instead, it is rather the hydrogen content which affects the mobility of the Li ions in these three systems, and in the following, we will analyze in greater detail the underlying mechanism for this behavior.

Figure 4 displays a visualization of the ion trajectories from our MD simulations for the systems in which *no* Li vacancy has been introduced. This helps to underline some of the findings described above, such as the increase of vibrational amplitudes with rising temperature and the onset of diffusion. But in addition, these plots are very useful in also showing the particular pathways that diffusing Li ions take in

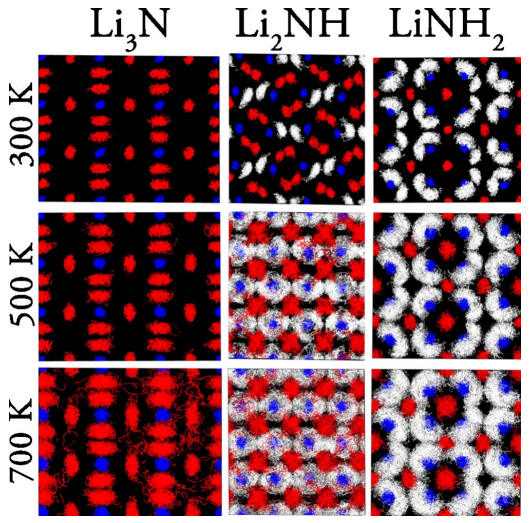

FIG. 4. (Color online) Ion trajectories in Li_3N, Li_2NH, and $LiNH_2$, projected into the *y*-*z* plane for 300, 500, and 700 K. The horizontal axis is aligned with the [001] direction while the vertical axis aligns with [010]. Trajectories are colored red, blue and white for Li, N, and H, respectively.

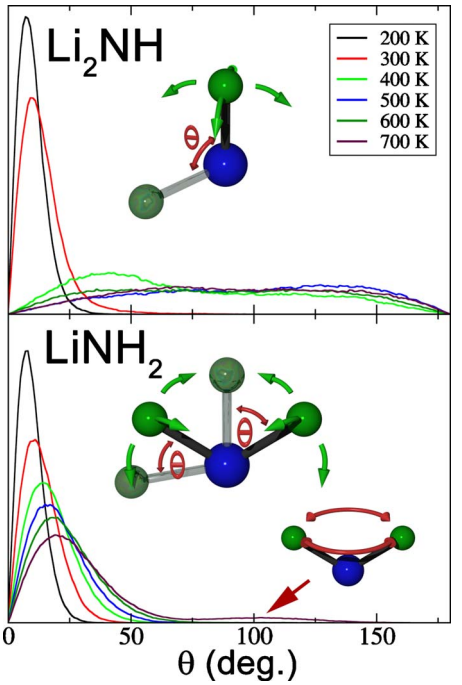

FIG. 5. (Color online) Bond orientation distribution plot for N–H bonds in Li_2NH (top panel) and $LiNH_2$ (bottom panel). The vertical height of the curves is proportional to how often during the MD simulation for a given temperature the orientation of any N–H bond deviated from its respective zero-temperature orientation by an angle θ plotted along the horizontal axis. Also, note that the number of possible configurations for a particular angle θ is proportional to sin θ. Hence, a completely random distribution of orientations would show up as a half-period of a sine curve, which can be seen to emerge for the higher temperature cases in Li_2NH. The respective insets illustrate the definition of θ, with the solid structures referring to the zero-temperature orientation and the slightly transparent one to an arbitrary example of a finite-temperature orientation (N in blue and H in green). It is also worth noting that in the case of $LiNH_2$, the slight elevation of the 700-K curve at around 100° corresponds to an exchange between the two N–H bonds in the NH_2 unit as illustrated in the second inset of the bottom panel.

the different materials. From a three-dimensional (3D) analysis, it becomes apparent that our results for Li_3N are in good agreement with previous findings[21,22,36] that showed Li to diffuse mainly within the Li_2N layers (triggered by the formation of a vacancy or Frenkel defect in the system with no vacancy), rarely crossing over from one Li_2N plane to another, and very little diffusion within the Li layers. Actually, below 700 K, Li diffusion is observed only for the supercell containing the Li vacancy, which shows that the ionic conductivity is controlled by the concentration of defects.

The trajectories plot also shows how the hydrogen atoms in Li_2NH and $LiNH_2$ possess a clear orientational preference at low temperatures, but as the temperature rises, they are seen to explore an increasingly larger space around the nitrogen atoms to which they are respectively bound. This behavior is actually even better captured in the form of a bond orientation distribution graph, shown in Fig. 5. As can be seen, in the case of Li_2NH at 200 and 300 K, the N–H bonds deviate only very slightly from their zero-temperature orien-

tation. But coinciding with the onset of Li diffusion at 400 K, the bond orientation distribution changes drastically, indicating that the N–H bonds are in fact accessing every possible angle (i.e., rotating 360° around) and no longer show any signs of the original orientational preference. For $LiNH_2$, the individual N–H bonds of the NH_2 units remain within close vicinity of the zero-temperature orientation (Fig. 5), merely vibrating back and forth within a confined angular range. As a consequence, only a gradual decrease in the peak amplitude (and a corresponding broadening of the peak) can be observed as the temperature rises. This behavior represents a very marked distinction from the sudden change seen for Li_2NH at 400 K. It thus seems that the full rotation of N–H bonds in Li_2NH is strongly linked to the promotion of Li mobility, while the absence of bond rotation in $LiNH_2$ is seen to be connected to the inhibition of Li mobility.

The presented findings can then be summarized and interpreted as follows. In Li_3N, the situation is most straightforward, with N staying fixed in place and Li starting to diffuse once the temperature is sufficiently high to have a Li atom overcome the energy barrier of leaving its equilibrium site. This creation of a Frenkel defect allows for adjacent Li atoms to hop there and take its place, and in turn allowing for new Li atoms to hop. If a vacancy is introduced *ad-hoc*, there is no need for the creation of a Frenkel defect, and the diffusion will start at much lower temperatures. As can be seen from the elevated MSD slope at 700 K in Li_3N with a vacancy [Fig. 1(d)], having both a created vacancy and Frenkel defects present, further enhances the Li diffusion.

A different situation is encountered in Li_2NH, where the mobility of Li is closely intertwined with the rotation of H. Below 400 K, the partially positively charged H atoms anchored to N in NH^{2-} need to orient in a certain way to minimize repulsion from nearby positively charged Li ions. But above 400 K, Li_2NH effectively transforms into a solid with rotationally disordered complex anions, in which the H atoms facilitate the diffusion mobility of the Li ions. When a vacancy is created, however, the anticipated increase in diffusion is absent.

Finally, yet another very different situation prevails in $LiNH_2$ where the NH_2^- units cannot rotate in the same manner as in Li_2NH to allow for Li to diffuse and, quite oppositely, effectively act as a hindrance instead. We believe this to be the underlying reason why Li is not exhibiting any mobility in $LiNH_2$ within the studied temperature range. If a vacancy is created, however, Li diffusion is found at 700 K. Simultaneously, we can also observe that the NH_2 units have started to rotate. The rotation is not as free as that of the NH units in Li_2NH, but rather a 180° rotation which swaps the position of the two hydrogen as schematically illustrated in the inset of the bottom panel in Fig. 5. This swapping motion gives rise to the trajectories plotted for $LiNH_2$ in Fig. 4.

In Li_3N, the nitrogen atoms carry essentially a charge of 3−, which results in a rather strong Coulomb attraction for the Li^+ ions. In addition, the relative abundance of Li leads to a situation where there is effectively less open space available for Li to move through the system. A high temperature of 700 K is therefore required for a Li atom to free itself from an equilibrium site, creating a Frenkel defect, and thus initiating the diffusion process of Li ions. In contrast to this, Li_2NH possesses only two Li per formula unit, the third having been replaced by a hydrogen atom, which is tightly bound to nitrogen. On the one hand, this results in a more open space for Li to move, and indeed we find Li diffusion onset at a comparatively low temperature of 400 K. On the other hand, at the same time, the charge state is reduced from 3− in N to 2− in NH and even further down to 1− in NH_2. By this simple argument alone, however, one would expect $LiNH_2$ to exhibit even higher Li mobility. Instead, we only find Li diffusion at 700 K when a vacancy has been created. To understand this counterintuitive behavior, one has to consider again the role played by the hydrogen atoms in the NH and NH_2 units. In Li_2NH, the concerted effort of the partially positively charged hydrogen atoms seems to actively promote the Li^+ diffusion through their respective N–H bond rotation by momentum transfer to Li ions, thus, helping them to overcome the energy barrier encountered in the diffusion process. By contrast, in $LiNH_2$, the two partially positively charged hydrogen atoms in each NH_2 unit cannot assist in the same manner, but instead they actually lead to "blockage," inhibiting the Li^+ diffusion, since it is not possible for two H atoms bound to N in the NH_2 unit to move in the same manner as a single H atom in an NH unit can.

Before arriving at the conclusions, we just want to briefly discuss one point pertaining to the Li mobility in Li_3N for the case when no Li vacancy was created *ad-hoc*. On the one hand, our results clearly indicate that Li self-diffusion in Li_3N does not commence until the temperature has reached 700 K. On the other hand, Li_3N is actually known to be a fast ion conductor, exhibiting high Li mobility even at room temperature. This does not mean, however, that there exists an actual discrepancy between our theoretical results and experimental data. Rather, the two refer to distinct scenarios due to different conditions. Li diffusion requires the creation of a Frenkel defect, and in reality, at finite temperature, there always exists a certain concentration of such defects, giving rise to the particular conductivities measured in experiment. Likewise, in our molecular dynamics study, Frenkel defects do occur. In Li_3N, the probability for their creation becomes high enough to encounter them within the simulation period once the temperature has reached 700 K. In other words, one has to keep in mind that due to the associated computational costs, we can only simulate an extremely tiny volume of the crystal for a very short time span. Under this aspect, it should not be at all surprising then that Li self-diffusion in Li_3N does not set in below 700 K if no vacancy is created. More meaningful is the comparison between the three Li-N-H systems (Li_3N, Li_2NH, and $LiNH_2$) and the prediction that the transition temperature to the superionic state is lower for Li_2NH compared to Li_3N.

IV. CONCLUSIONS

We have demonstrated through first-principles calculations that the stepwise hydrogenation of Li_3N results in two very different scenarios, namely one in which hydrogen acts as a *promoter* and one in which it acts as an *inhibitor* of the superionic state. Thus, in Li_2NH, we find that the partially positively charged hydrogen atoms of the rotationally disor-

dered NH units actively facilitate the mobility of the Li^+ ions, while contrary to that in $LiNH_2$, the NH_2 units cannot rotate in the same manner and ultimately hinder the Li mobility instead. The effect of Li vacancies plays different roles in the three system. In Li_3N and $LiNH_2$, the creation of Li vacancies can actually promote the diffusion process, while in Li_2NH, the creation of vacancies is not seen to affect the diffusion process. This tells us that the rate limiting factor for the Li diffusion changes from the creation of vacancies to the rotation of NH units as hydrogen is added. While the studied materials have lately received much attention for their role as hydrogen storage systems, we believe that our findings regarding the effect of the hydrogenation level on the lithium ion conductivity could also prove quite useful for a broad range of materials research related to battery and fuel cell applications.

Finally, we would like to draw attention again to a very recent investigation[23] of $LiNH_2$ and Li_2NH which used both theory and experiment (in the form of ^1H NMR measurements) to show that Li atoms in the amide and imide systems possess higher mobility and are more disordered than what can be expected based on data obtained from x-ray scattering. Such a conclusion is in line with our earlier stated view[24] that time-averaging measurements, such as x-ray or neutron scattering, will show a well-ordered simple-cubic structure for the cation sublattice in Li_2NH, neglecting to detect the superionic state, which could be experimentally observed through measurements of the ionic conductivity.

ACKNOWLEDGMENTS

The authors thank the Swedish Foundation for International Cooperation in Research and Higher Education (STINT), the Swedish Research Council (VR), Formas, Futura Foundation, Wenner-Gren Foundations, the National University of Singapore, and the Dalian Institute of Chemical Physics for financial support. Both the Swedish National Infrastructure for Computing (SNIC) and the Uppsala Multidisciplinary Center for Advanced Computational Science (UPPMAX) provided computing time for this project.

*Corresponding author; rajeev.ahuja@fysik.uu.se

[1] R. Juza and K. Opp, Z. Anorg. Allg. Chem. **266**, 325 (1951).
[2] R. Juza and K. Opp, Z. Anorg. Allg. Chem. **266**, 313 (1951).
[3] P. Chen, Z. Xiong, J. Luo, J. Lin, and K. L. Tan, Nature (London) **420**, 302 (2002).
[4] T. Ichikawa, N. Hanada, S. Isobe, H. Leng, and H. Fujii, J. Phys. Chem. B **108**, 7887 (2004).
[5] K. Miwa, N. Ohba, S. I. Towata, Y. Nakamori, and S. I. Orimo, Phys. Rev. B **71**, 195109 (2005).
[6] J. F. Herbst and L. G. Hector, Jr., Phys. Rev. B **72**, 125120 (2005).
[7] T. Noritake, H. Nozaki, M. Aoki, S. Towata, G. Kitahara, Y. Nakamori, and S. Orimo, J. Alloys Compd. **393**, 264 (2005).
[8] K. Ohoyama, Y. Nakamori, S. Orimo, and K. Yamada, J. Phys. Soc. Jpn. **74**, 483 (2005).
[9] B. Magyari-Köpe, V. Ozoliņš, and C. Wolverton, Phys. Rev. B **73**, 220101(R) (2006).
[10] M. P. Balogh, C. Y. Jones, J. F. Herbst, L. G. Hector, Jr., and M. Kundrat, J. Alloys Compd. **420**, 326 (2006).
[11] C. Moysés Araújo, R. H. Scheicher, P. Jena, and R. Ahuja, Appl. Phys. Lett. **91**, 091924 (2007).
[12] C. Moysés Araújo, R. H. Scheicher, and R. Ahuja, Appl. Phys. Lett. **92**, 021907 (2008).
[13] M. S. Dresselhaus and I. L. Thomas, Nature (London) **414**, 332 (2001).
[14] J. S. Rigden, *Hydrogen: The Essential Element* (Harvard University Press, Cambridge, MA, 2003).
[15] W. Grochala and P. P. Edwards, Chem. Rev. **104**, 1283 (2004).
[16] J. Alper, Science **299**, 1686 (2003).
[17] R. D. Cortright, R. R. Davda, and J. A. Dumesic, Nature (London) **418**, 964 (2002).
[18] N. L. Rosi, J. Eckert, M. Eddaoudi, D. T. Vodak, J. Kim, M. O'Keeffe, and O. M. Yaghi, Science **300**, 1127 (2003).
[19] L. Schlapbach and A. Züttel, Nature (London) **414**, 353 (2001).
[20] L. Schlapbach, Nature (London) **460**, 809 (2009).
[21] M. L. Wolf, J. R. Walker, and C. R. A. Catlow, J. Phys. C **17**, 6623 (1984).
[22] M. L. Wolf and C. R. A. Catlow, J. Phys. C **17**, 6635 (1984).
[23] G. A. Ludueña, M. Wegner, L. Bjålie, and D. Sebastiani, ChemPhysChem **11**, 2353 (2010).
[24] C. Moysés Araújo, A. Blomqvist, R. H. Scheicher, P. Chen, and R. Ahuja, Phys. Rev. B **79**, 172101 (2009).
[25] W. Kohn and L. J. Sham, Phys. Rev. **140**, A1133 (1965).
[26] G. Kresse and J. Furthmüller, Comput. Mater. Sci. **6**, 15 (1996).
[27] G. Kresse and D. Joubert, Phys. Rev. B **59**, 1758 (1999).
[28] H. Gunaydin, K. N. Houk, and V. Ozoliņš, Proc. Natl. Acad. Sci. U.S.A. **105**, 3673 (2008).
[29] H. Lee, D. Kim, N. Singh, M. Kołaski, and K. Kim, J. Chem. Phys. **127**, 164311 (2007).
[30] N. A. Zarkevich and D. D. Johnson, Phys. Rev. Lett. **100**, 040602 (2008).
[31] D. E. Farrell, Dongwon Shin, and C. Wolverton, Phys. Rev. B **80**, 224201 (2009).
[32] J. P. Perdew and Y. Wang, Phys. Rev. B **45**, 13244 (1992).
[33] P. E. Blöchl, Phys. Rev. B **50**, 17953 (1994).
[34] A. Huq, J. W. Richardson, E. R. Maxey, D. Chandra, and W. M. Chien, J. Alloys Compd. **436**, 256 (2007).
[35] J. B. Yang, X. D. Zhou, Q. Cai, W. J. James, and W. B. Yelon, Appl. Phys. Lett. **88**, 041914 (2006).
[36] J. Sarnthein, K. Schwarz, and P. E. Blöchl, Phys. Rev. B **53**, 9084 (1996).